Journal of Hazardous Materials 168 (2009) 901–908

Contents lists available at ScienceDirect

Journal of Hazardous Materials

journal homepage: www.elsevier.com/locate/jhazmat

Heterogeneous photo-Fenton photodegradation of reactive brilliant orange X-GN over iron-pillared montmorillonite under visible irradiation

Qiuqiang Chen, Pingxiao Wu*, Yuanyuan Li, Nengwu Zhu, Zhi Dang

College of Environmental Science and Engineering, South China University of Technology, Guangzhou, 510006, PR China

ARTICLE INFO

Article history:
Received 14 November 2008
Received in revised form 13 January 2009
Accepted 19 February 2009
Available online 3 March 2009

Keywords:
Heterogeneous photo-Fenton
Iron-pillared montmorillonite
Visible light irradiation
Reactive brilliant orange

ABSTRACT

Decolorization and mineralization of reactive brilliant orange X-GN was investigated under visible light irradiation ($\lambda \geq 420$ nm) by using Fe-Mt/H_2O_2 as the heterogeneous photo-Fenton reagent. The characterization results (XRD, FTIR, XRF, BET, XPS, UV–vis diffuse spectra) of Fe-Mt suggested that small-sized hydrolyzed iron successfully intercalated into the interlayer spaces of the clay via pillaring. The stability of the Fe-Mt catalyst was evaluated according to the decolorization efficiency for X-GN with used catalyst from previous runs and the concentration of iron ions leached from the solid structure into the reaction solution. The catalytic results showed that at a reaction temperature of 30 °C, pH 3.0, 4.9 mmol/L H_2O_2 and 0.6 g/L catalyst dosage, 98.6% discoloration and 52.9% TOC removal of X-GN were achieved under visible irradiation after 140 min treatment. Furthermore, the maximum concentration of dissolved iron ions was 1.26% of the total iron content in the Fe-Mt catalyst after photocatalysis. A halogen lamp as light source has demonstrated that visible radiation can be successfully used for a heterogeneous photo-Fenton process.

1. Introduction

Over 700,000 t of approximately 10,000 types of dyes and pigments are produced every year worldwide. From this amount, about 20% are discharged without treatment [1]. Dyeing wastewater contains considerable color, is generally toxic and is recalcitrant to conventional physical, chemical, and biological wastewater treatment processes [2,3]. In order to develop an efficient process and to solve problems of the traditional methods for dye wastewater treatment, advanced oxidation processes (AOPs) are widely applied, as these generate highly reactive OH radicals, which are known as strong and non-selective oxidizers of the organic matter in dye water [4]. Among the AOPs is the Fenton reaction, a mixture of hydrogen peroxide and iron salt (homogeneous or heterogeneous), with or without light assistance (the so-called photo-Fenton process or Fenton process).

However, the homogeneous Fenton system that employs iron salt in the form of ferric solution is inappropriate, because it leads to a high iron concentration in the final effluent so that the removal of the sludge containing Fe ions is expensive in labor, reagents and time [5]. Thus, efforts have been made to find efficient heterogeneous iron catalysts, including mixed oxides of iron and silica [6], iron exchanged zeolite [7,8], and iron-pillared clays [9,10]. Being inexpensive and widely available, iron-pillared montmorillonitic clay as catalyst has received considerable recognition [11]. Recently, a number of studies have found that montmorillonitic clay containing iron could be used in heterogeneous photo-Fenton catalysis [12]. Chen *et al* have investigated the heterogeneous UV/Fenton catalytic degradation of dyestuff by using hydroxyl-Fe pillared bentonite. Their results indicated that almost 100% decolorization and more than 65% TOC removal of Acid Light Yellow G was achieved after 120 min treatment [13].

Attention has been focused on the application of a heterogeneous photo-Fenton process to the photodegradation of reactive dye wastewater under UV irradiation. However, the ultraviolet band occupies only 3–5% of the solar light energy that reaches the earth, while artificial ultraviolet apparatus typically consumes large quantities of electrical power,which limits industrial application [14]. Therefore, it is accepted that an important issue in the heterogeneous photo-Fenton process is to develop catalysts which efficiently use sunlight or visible light irradiation instead of UV as the light source. Particularly as energy has recently increased in price, the ability to utilize visible light or sunlight for dye wastewater treatment is a priority. Cheng *et al* have reported that the exchangeable interlayer iron ions in clays such as montmorillonite, laponite and nontronite had good catalytic performance for photodegradation of organic dyes under visible irradiation [15].

In this study, we investigated photocatalytic degradation of X-GN by Fe-Mt/H_2O_2 under visible irradiation ($\lambda \geq 420$ nm) which was given off by a halogen lamp and analyzed the effects of reaction conditions, such as X-GN concentration, solution pH, catalyst dosage and reaction temperature, on the decolorization of X-GN.

* Corresponding author. Tel.: +86 20 39380538; fax: +86 20 39383725.
E-mail address: pppxwu@scut.edu.cn (P. Wu).

0304-3894/$ – see front matter © 2009 Elsevier B.V. All rights reserved.
doi:10.1016/j.jhazmat.2009.02.107

Table 1
Chemical Compositions of Mt and Fe-Mt Determined by XRF.

Element	Concentration (wt%)		Element	Concentration (wt%)	
	Mt	Fe-Mt		Mt	Fe-Mt
O	50.8	55.3	Fe	2.07	11.2
Mg	1.86	1.07	Ti	0.08	0.04
Si	32.4	19.0	K	0.09	0.05
Na	0.72	0.56	N	1.56	8.39
Ca	1.70	0.01	Al	6.75	4.40

In addition, comparison of heterogeneous photo-Fenton and visible light/H_2O_2/Fe^{3+} processes with color and TOC removal was also performed. The results will help realize the photocatalytic properties of Fe-Mt which can utilize visible light or solar light for industrial applications.

2. Experimental section

2.1. Chemicals and reagents

The montmorillonite (Mt) was from a bentonite deposit in Heping (Guangdong, PRC). Its chemical composition as determined by X-ray fluorescence analysis is shown in Table 1.

Reactive brilliant orange X-GN (hereafter, X-GN) was purchased from Advanced Technology Industry Ltd. (Hong Kong, PRC) as a commercially available dye and used without further purification. The chemical structure of X-GN is shown as Fig. 1. Hydrogen peroxide (30% volume solution), ferric nitrate, sulfuric acid and sodium carbonate were of analytical grade and obtained from the Guangzhou Chemical Reagent Factory (Guangzhou, PRC). De-ionized water was used throughout this experiment.

2.2. Catalyst preparation

The preparation of the Fe-Mt catalyst [16] was as follows: First, sodium carbonate was added slowly as powder into a vigorously stirred 0.2 M solution of iron nitrate while stirring for 2 h at room temperature so that a molar ratio of 0.75:1 for Na^+/Fe^{3+} was established. The solution was then aged at 30 °C for 24 h. Second, an aqueous dispersion of montmorillonite was prepared by adding 2 g of clay to 100 mL water while stirring vigorously. Finally, the solution from the first step was added into the dispersed montmorillonite clay. The proportion of iron cations to clay was 10 mmol Fe^{3+} per gram of clay. The product was then filtered, washed with de-ionized water several times, dried at 80 °C for 24 h, ground to 200-mesh and named as Fe-Mt.

2.3. Photocatalysis reaction setup

Experimental investigations were carried out in a 500 mL double glass cylindrical jacket reactor (20 cm inner length, 10 cm inner diameter) with 200 mL X-GN solution, as shown in Fig. 2. The reactor was maintained at a fixed temperature, which was controlled

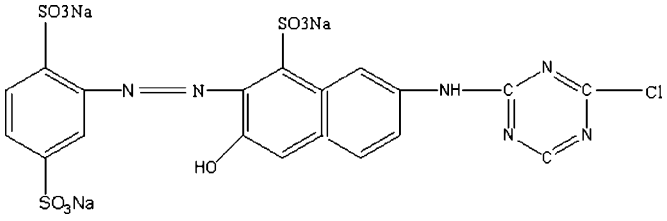

Fig. 1. Chemical structure of reactive brilliant orange X-GN.

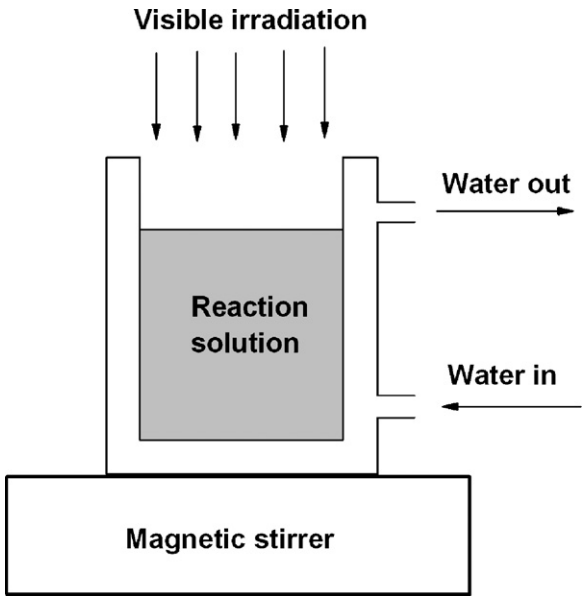

Fig. 2. Schematic diagram of photo-catalytic reactor used in this study.

by circulating water to within ±0.5 °C. The visible irradiation source was a Philips 300 W halogen lamp with a cutoff filter to filter out the light of wavelengths below 420 nm. The light intensity which reached the reaction solution surface was 42300 ± 200 lx, detected using a Tenmars DL-201 digital illuminometer. The initial pH value of the solution was adjusted by adding NaOH or H_2SO_4.

The heterogeneous photo-Fenton process was conducted as follows: After pH adjustment, a given amount of Fe-Mt catalyst was added into the solution of 200 mL X-GN, and was stirred vigorously in darkness for 10 min in order to estimate the adsorption of the dye on the photocatalyst surface (the adsorption period) and then turned off the halogen lamp and added hydrogen peroxide. This point was taken as the initial time for the experiments (the photo-oxidation period). Samples were taken from the irradiated solutions at various times during photolysis, followed by filtration through a 0.45 μm filter membrane to separate the solid from the liquid before measurement.

A set of control experiments to study the performance of other processes (including visible light only, Fe-Mt only, visible light/Fe-Mt, visible light/H_2O_2, visible light/H_2O_2/Mt, H_2O_2/Fe-Mt in darkness (Fenton)) and visible light/H_2O_2/Fe^{3+} on the decolorization of X-GN was also investigated.

2.4. Analytical procedure

2.4.1. Characterization of the catalysts

The X-ray diffraction (XRD) patterns of the catalysts (before and after preparation) were measured with a Rigaku D/MAX-IIIA X-ray diffractometer equipped with Cu Kα radiation. Sample spectra were recorded by the KBr pellet technique on a PerkinElmer 1725X Fourier transform infrared spectrometer. The chemical compositions of the samples were analyzed by a PANalytical PW-4400 X-ray fluorescence spectrometer (XRF). Specific surface areas were determined by adsorption of nitrogen at 77 K on a Micromeritics ASAP 2020 surface area and porosity analyzer. X-ray photoelectron spectra was measured by an ANELVA AES-430S X-ray photoelectron spectrometer and the BE of C 1s was shifted to 284.6 eV as an internal reference. The pass energy was 40 eV and a conventional Al Kα anode radiation source was used as the excitation source. UV–vis diffuse spectra were recorded by a Shimadzu 2501 PC UV–vis spectrophotometer. The reference was $BaSO_4$.

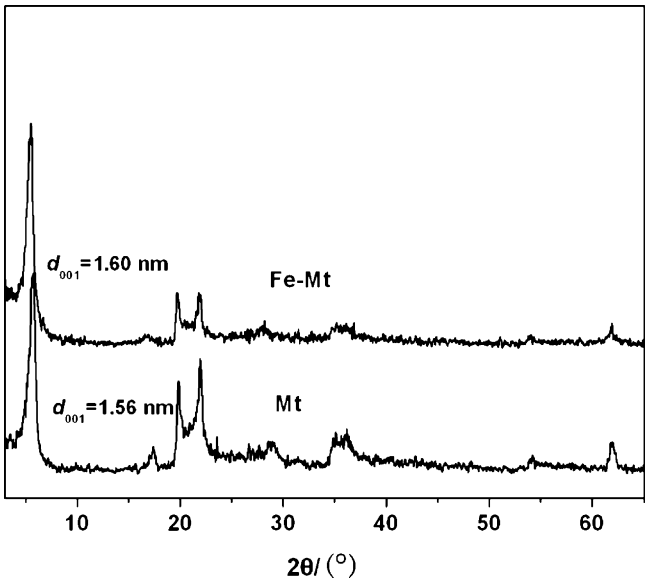

Fig. 3. XRD patterns of the samples.

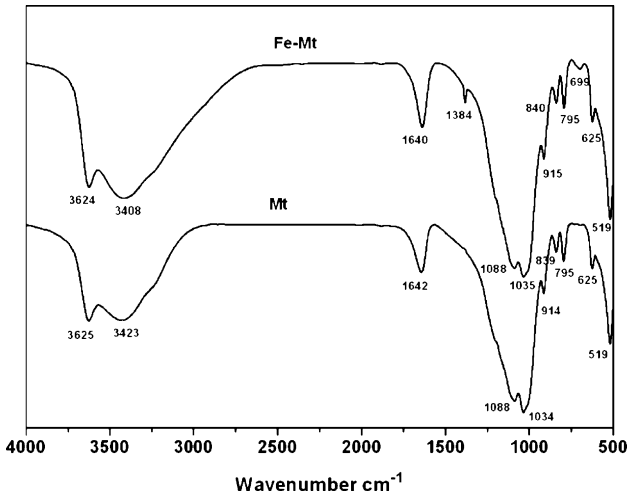

Fig. 4. FT-IR spectra of the samples.

2.4.2. Reaction solution analysis

The pH value of the solutions was determined using a PHS-3C pH meter. The UV–vis spectrum of X-GN was measured with a Shimazu 2450 UV–vis spectrophotometer. Prior to measurement, a calibration curve was obtained using standard X-GN solutions with known concentrations. The decolorization efficiency of X-GN was determined by the following expression:

$$E(\%) = \frac{C_0 - C}{C_0} \times 100 \quad (1)$$

where C and C_0 denote to the time-dependent concentration and the initial concentration, respectively.

Total organic carbon (TOC) concentration during photolysis was carried out in a Shimadzu TOC-500 analyzer to evaluate the mineralization of X-GN. The mineralization efficiency of the dye was also defined as per (Eq. (1)), where C is the value of TOC obtained at time t and C_0 corresponds to the initial value of TOC. The concentrations of iron ions leached from the catalyst into the reaction solution at different time were measured by Zeeman 2000 atomic absorption spectrophotometer (AAS).

3. Results and discussion

3.1. Catalyst characterization

The d_{001} reflection is the main source used to identify the clays. In the sample XRD patterns (as is shown in Fig. 3), we can see that the d_{001} basal spacing increased from 1.56 nm (Mt) to 1.60 nm (Fe-Mt), confirming the intercalation of some small-sized hydrolyzed iron in the interlayer spaces of the clay particles via pillaring. Additionally, compared to the unpillared Mt, those peaks of the Fe-Mt are less prominent and some peaks have disappeared, which indicates the ordered layered structure of Fe-Mt was subjected to some disruption. This disruption possibly arises from the pillaring process, since Na^+ and Ca^{2+} are exchanged by hydrolyzed iron, as can be confirmed from Table 1.

FTIR spectra (500–4000 cm^{-1}) of the Mt and Fe-Mt samples are presented in Fig. 4. Comparing the spectrum of pure Mt with the spectrum of Fe-Mt, two new peaks emerged at 1384 cm^{-1} and 699 cm^{-1}. The former was the NO_3^- stretching mode, which showed that there were some redundant positively-charged iron aggregates outside the interlayer space of Fe-Mt [17], while the latter was the FeOOH bending vibration, which also suggested that hydrolyzed iron intercalated into interlayers proceeded by pillaring.

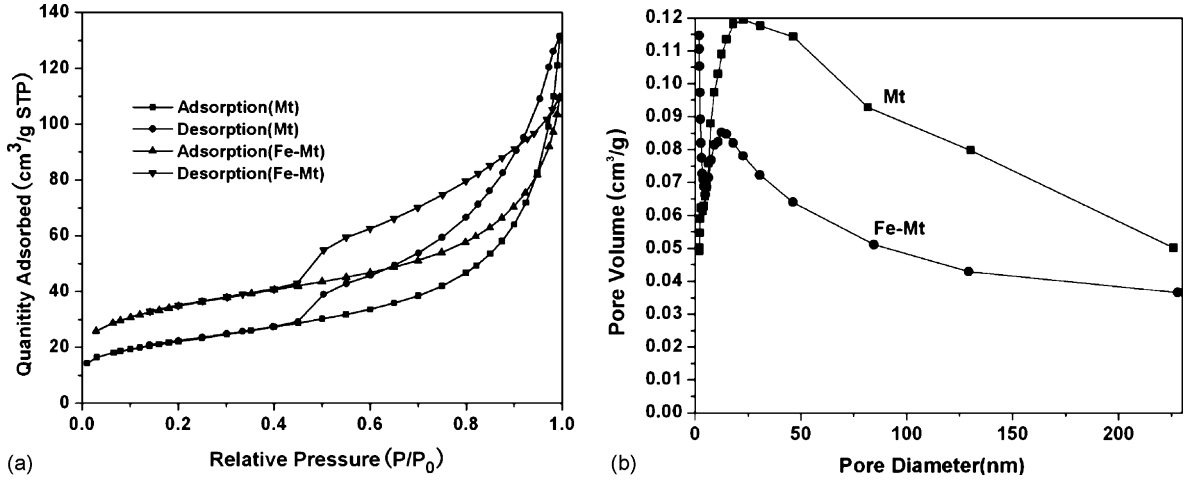

Fig. 5. (a) Nitrogen adsorption–desorption isotherms of the samples, (b) BJH pore size distributions of the samples.

Table 2
Textural parameters and basal spacing for the samples.

Sample	BET surface area (m^2/g)	Pore volume (cm^3/g)	Pore size (nm)	d_{001} (nm)
Mt	78.5	0.153	7.81	1.56
Fe-Mt	122.8	0.142	4.63	1.60

Table 3
Binding energy of Fe-Mt determined by XPS.

Element	Binding energy (eV)	Element	Binding energy (eV)
C 1s	284.6	Fe 2p	711.6
O 1s	531.6	Si 2p	102.6
Al 2p	73.6	Ca 2p	350.6

The chemical composition of the samples was measured by XRF and is shown in Table 1. The results revealed that the Fe concentration of the Fe-Mt catalyst is 11.2 wt%, while it is only 2.07 wt% in Mt. Fe was introduced into the clay layers after pillaring. The specific surface area, pore volume of and pore size of Fe-Mt were 122.8 m^2/g, 0.142 cm^3/g and 4.63 nm, whereas they were 78.5 m^2/g, 0.153 cm^3/g and 7.81 nm in Mt. Fig. 5a displays the nitrogen adsorption–desorption isotherms of Mt and Fe-Mt. It is evident that Fe-Mt showed significant adsorption at very low relative pressures, characteristic of microporous solids [11]. Therefore, the more than 50% increase in the BET surface area in Fe-Mt was a result of the pillaring of the clay with a consequent increasing in the number of micropores (as is shown in Fig. 5b), while the pore volume and pore size became smaller, as can be seen from Table 2.

The major XPS results are presented in Table 3 and Fig. 6. The binding energy of the Fe in Fe-Mt catalyst was determined to be 711.6 eV (Table 3), which indicates that the oxidation status of Fe was mostly Fe^{3+} ions and no Fe in a zero oxidation state was detected [12]. Compared to the pure Mt, the intensity of Fe 2p in Fe-Mt was enhanced markedly (Fig. 6). This is indicative of Fe(III) species growth during pillaring. The UV–vis diffuse reflectance spectra of the samples are shown in Fig. 7. It can be seen that the Fe-Mt catalyst showed a significant absorption in visible light region up to 600 nm, in contrast to the absorption edges at about 400 nm in pure Mt.

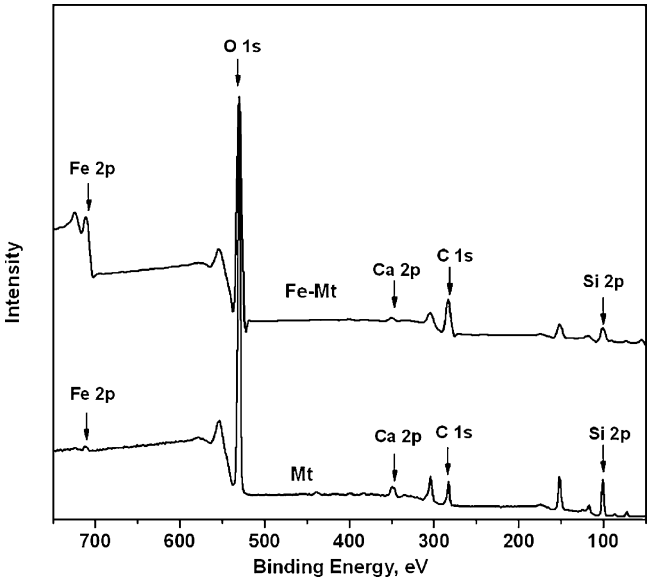

Fig. 6. X-ray photoelectron spectra of the samples.

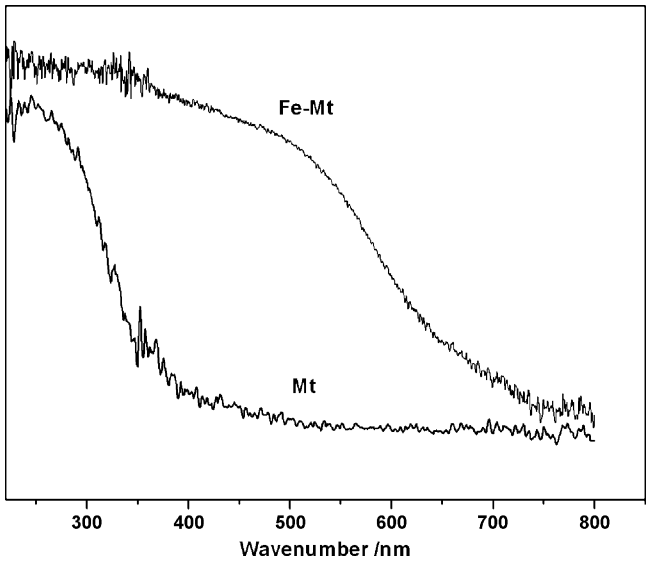

Fig. 7. UV–vis diffuse reflectance spectra of the samples.

3.2. Photo-catalytic activity of iron-pillared montmorillonite catalyst

3.2.1. Comparison of process reactants

Decolorization of X-GN by visible light only, visible light/H_2O_2, visible light/Fe-Mt, visible light/H_2O_2/Mt, visible light/H_2O_2/Fe^{3+}, H_2O_2/Fe-Mt in darkness (Fenton) and visible light/H_2O_2/Fe-Mt (heterogeneous photo-Fenton) were carried out; the results are shown in Fig. 8. It is clear to see that X-GN was resistant to photolysis under visible irradiation only or combined with H_2O_2. The decolorization efficiency under visible irradiation alone (curve a) was 1.3%, while it was 8.8% with irradiation and H_2O_2 (curve b). For visible light/Fe-Mt (curve c), color removal of X-GN was increased to 11.5%. It can be attributed to two aspects: on the one hand, the Fe-Mt can act as a heterogeneous catalyst under visible irradiation, generating a bit OH radicals that attacked the dye X-GN; on the

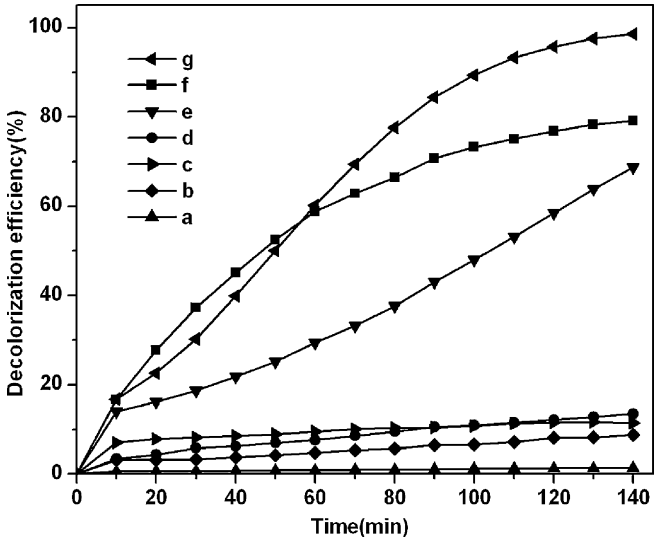

Fig. 8. Decolorization of X-GN by different processes: (a) visible irradiation only, (b) with 4.9 mmol/L H_2O_2 and visible irradiation, (c) with 0.6 g/L Fe-Mt and visible irradiation, (d) with 0.6 g/L Mt, 4.9 mmol/L H_2O_2, and visible irradiation, (e) with 0.6 g/L Fe-Mt, 4.9 mmol/L H_2O_2 in the dark, (f) with 0.84 ppm Fe^{3+}, 4.9 mmol/L H_2O_2, and visible irradiation, (g) with 0.6 g/L Fe-Mt, 4.9 mmol/L H_2O_2, and visible irradiation. The experiments were conducted under conditions: [X-GN] = 100 mg/L, pH 3, T = 30 °C.

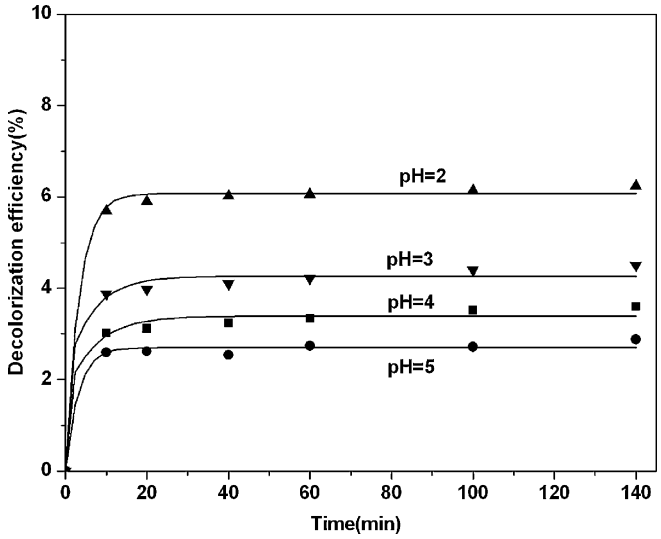

Fig. 9. pH effect for the adsorption of X-GN on the surface of Fe-Mt without visible irradiation. The experimental conditions were conducted under conditions: [X-GN] = 100 mg/L, Fe-Mt = 0.6 g/L, T = 30 °C.

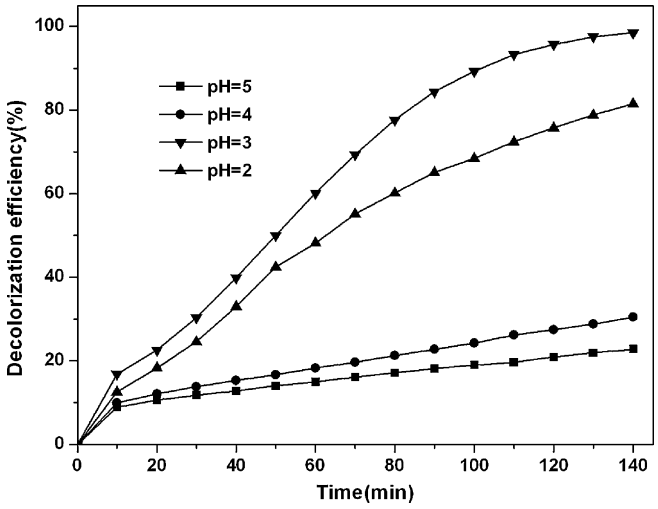

Fig. 10. Effect of initial pH on the decolorization of X-GN by heterogeneous photo-Fenton process. The experimental conditions were conducted under conditions: [X-GN] = 100 mg/L, $[H_2O_2]_0$ = 4.9 mmol/L, Fe-Mt = 0.6 g/L, T = 30 °C.

other hand, the adsorption of X-GN on the surface of Fe-Mt catalyst led to a limiting color removal (as is shown in Fig. 9). In the visible light/H_2O_2/Mt system (curve d), color removal of X-GN was just a bit higher than that in visible light/H_2O_2 system (curve b), and the decolorization efficiency was 13.5%. This indicates that the pure Mt is not a good heterogeneous catalyst. When the reaction was carried out in visible light/H_2O_2/Fe-Mt (this is the so-called heterogeneous photo-Fenton process, curve g), great enhancement of the decolorization rate was observed, and 98.6% color removal was achieved. Such enhancement was due to large amount of OH radicals generated from the reactions (2)–(5) and (11) [15,18–20]. In contrast, without visible irradiation, but with H_2O_2 and Fe-Mt in darkness (curve e), color removal ratio was decreased to 68.7% after 140 min treatment (Eqs. (6), (7), (10)) [15,20], illustrating that the decolorization rate can be accelerated by using visible radiation as light source.

$$H_2O_2 + \text{visiblelight} \rightarrow {}^{\bullet}OH + OH^- \quad (2)$$

$$\text{X-GN} + \text{visiblelight} \rightarrow \text{X-GN}* \quad (3)$$

$$\text{Fe(III)species} + \text{X-GN}* \rightarrow \text{Fe(II)species}(e^-) + \text{X-GN}^{+\bullet} \quad (4)$$

$$H_2O_2 + \text{Fe(II)species}(e^-) \rightarrow {}^{\bullet}OH + \text{Fe(III)species} \quad (5)$$

$$\text{Fe(III)species} + H_2O_2 \rightarrow \text{Fe(II)species} + HO_2{}^{\bullet} + H^+ \quad (6)$$

$$\text{Fe(II)species} + {+}H_2O_2 \rightarrow \text{Fe(III)species} + {}^{\bullet}OH + OH^- \quad (7)$$

$$\text{X-GN}* + Fe^{3+} \rightarrow Fe^{2+} + \text{X-GN}^{+\bullet} \quad (8)$$

$$Fe^{2+} + H_2O_2 \rightarrow Fe^{3+} + OH^- + {}^{\bullet}OH \quad (9)$$

$${}^{\bullet}OH + \text{X-GN} \rightarrow \text{X-GNdegradedproducts} \quad (10)$$

$${}^{\bullet}OH + \text{X-GN}^{+\bullet} \rightarrow \text{X-GNdegradedproducts} \quad (11)$$

It can be observed that 79.1% decolorization (curve f) of the dye took place under visible irradiation of 140 min with 0.84 ppm Fe^{3+} ions (by adding $Fe(NO_3)_2{\cdot}9H_2O$ into the X-GN solution.) as a homogeneous catalyst in the presence of H_2O_2 (Eqs. (2), (3), (8), (9), (11))) [15,18,20,21]. We can also find that its decolorization efficiency was 19.5% less than that in heterogeneous photo-Fenton process. Furthermore, it should be pointed out that because the concentrations of dissolved iron were far lower than 0.84 ppm during the photolysis except that at 140 min (Fig. 16), the actual degradation of X-GN by the dissolved iron ions should be much less than that with 0.84 ppm Fe^{3+} ions. Therefore, the heterogeneous photo-Fenton process with Fe-Mt as catalyst played a dominant role in the photolysis of X-GN.

3.2.2. Effect of the initial pH on the decolorization of X-GN

The pH of the solution plays an important role in decolorizing dyes in the photo-Fenton process [22]. A set of experiments was performed to determine the effect of initial solution pH, for pH between 2 and 5, on the discolorization of X-GN. As is shown in Fig. 10, the decolorization of X-GN is markedly affected by the initial pH. For example, the final decolorization efficiency increased from 22.8% to 98.6% if the pH was decreased from 5 to 3. However, decolorization efficiency of X-GN was reduced to 81.5% at 140 min when the initial pH was decreased to 2. This is due to the formation of $H_3O_2{}^+$, which enhanced the stability of H_2O_2 and inhibited the generation of OH radicals when the pH was less than 3.0 [23]. In addition, a pH lower than 3 favors leaching of the metal into the solution [24]. Based on the observed effect of pH, pH 3 was chosen as the optimum pH in this heterogeneous photo-Fenton process for further experiments.

3.2.3. Effect of catalyst dosage on the decolorization of X-GN

The effect of Fe-Mt dosage on the decolorization was investigated by varying the Fe-Mt dosage from 0.1 to 1 g/L. It can be seen from Fig. 11 that the decolorization efficiency increased with the catalyst dosage up to 0.6 g/L, and then slightly decreased upon further addition of the catalyst. It is believed that Fe-Mt functions as a heterogeneous catalyst that can accelerate the decomposition of H_2O_2 and more OH radicals are produced with increase of Fe-Mt dosage. However, Fe-Mt particles make the reaction solution very turbid when the dosage of Fe-Mt was high, so that the penetration of visible light was diminished, hindering the generation of OH radicals [25]. A suitable catalyst dosage for the decolorization of X-GN by heterogeneous photo-Fenton process under visible irradiation is 0.6 g/L at the concentration of the dye and H_2O_2 employed.

3.2.4. Effect of the hydrogen peroxide dosage on the decolorization of X-GN

The influence of different concentrations of H_2O_2 on the decolorizing of X-GN in the heterogeneous photo-Fenton process was investigated. As is shown in Fig. 12, with increasing concentration of H_2O_2 from 2.9 to 9.8 mmol/L, the degradation efficiency of X-GN went up from 65.4% to 95.6% at 90 min. The enhancement of decolorization rate by addition of H_2O_2 is due to increase in OH radicals. However, it should be pointed out that when the concentration of

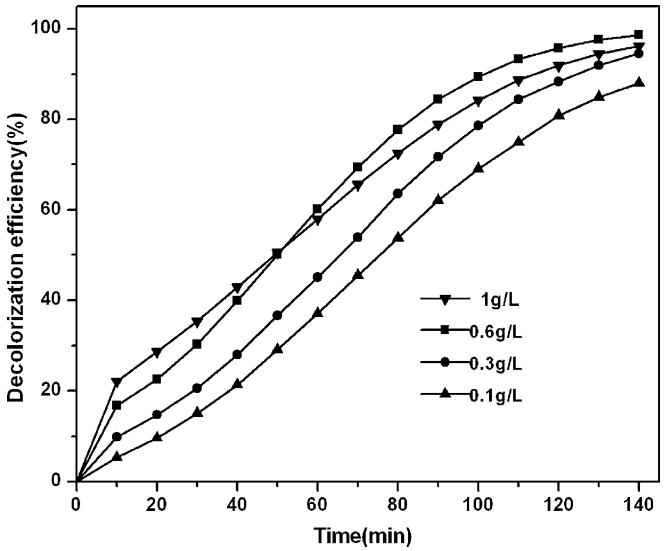

Fig. 11. Effect of Fe-Mt dosage on the decolorization of X-GN by heterogeneous photo-Fenton process. The experiments were conducted under conditions: [X-GN] = 100 mg/L, $[H_2O_2]_0$ = 4.9 mmol/L, pH 3, T = 30 °C.

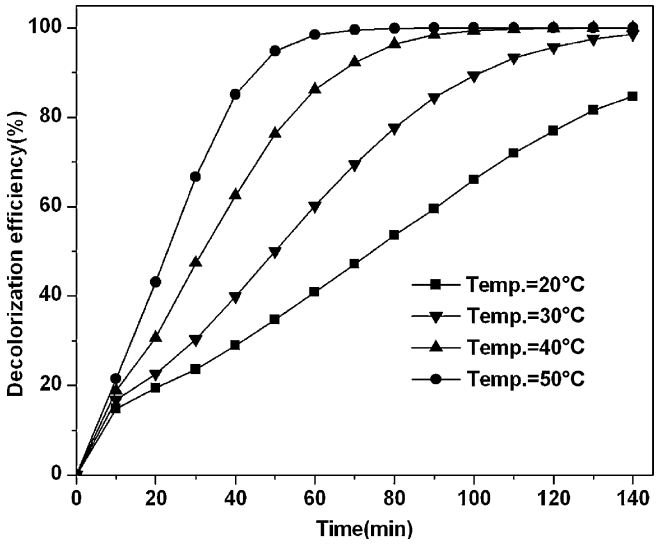

Fig. 13. Effect of temperature on the decolorization of X-GN by heterogeneous photo-Fenton process. The experiments were conducted under conditions: [X-GN] = 100 mg/L, $[H_2O_2]_0$ = 4.9mmol/L, Fe-Mt = 0.6 g/L, pH 3.

H_2O_2 was over 9.8 mmol/L, the removal of X-GN decreased slightly. This can be explained by the scavenging of OH radicals at a higher concentration of H_2O_2, leading to decrease in the number of OH radicals in solution (Eqs. (12) and (13)) [26].

$$H_2O_2 + {}^{\bullet}OH \rightarrow H_2O + {}^{\bullet}HO_2 \quad (12)$$

$$^{\bullet}HO_2 + {}^{\bullet}OH \rightarrow H_2O + O_2 \quad (13)$$

Hence, a dosage of 4.9 mmol/L H_2O_2 can be used as the optimum dosage for the decolorization of X-GN.

3.2.5. Effect of temperature on the decolorization of X-GN

Prior to the experiments studying the effect of temperature on color removal of X-GN in heterogeneous photo-Fenton process, a blank experiment was carried out to elucidated the decomposition of the dye with elevated temperature from 20 to 50 °C under visible irradiation at pH 3 without Fe-Mt and H_2O_2. It was found that the decomposition of X-GN by elevating temperature was nearly negligible, with a maximum decolorization efficiency of 1.7% at T = 50 °C whereas a lowest value of 0.9% at T = 20 °C at 140 min. So the dye is concluded to be stable. Fig. 13 depicts the influence of temperature in the range of 20–50 °C on the decolorizing of X-GN in heterogeneous photo-Fenton process. Obviously, higher temperature accelerated the decolorization of X-GN in the presence of Fe-Mt and H_2O_2 under visible irradiation because the rate of generation of OH radicals increased with elevated temperature [27]. For example, when the reaction temperature was increased from 20 to 50 °C, the color removal efficiency increased from 40.9% to 98.4% after 140 min irradiation.

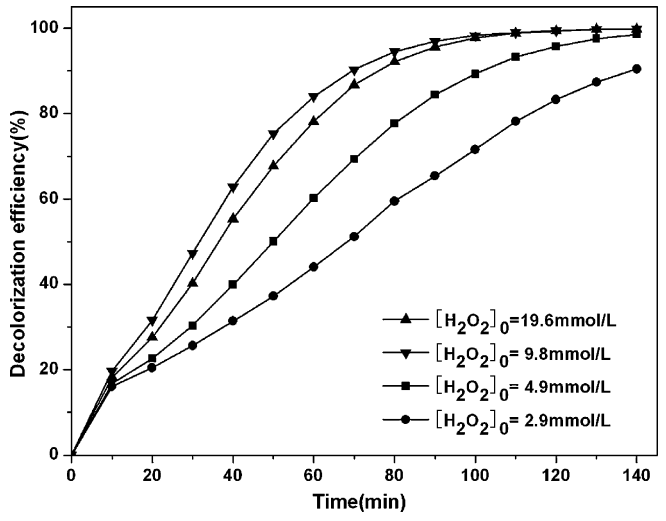

Fig. 12. Effect of H_2O_2 dosage on the decolorization of X-GN by heterogeneous photo-Fenton process. The experiments were conducted under conditions: [X-GN] = 100 mg/L, Fe-Mt = 0.6 g/L, pH 3, T = 30 °C.

3.2.6. Comparative decolorization and mineralization of X-GN

Decolorization does not mean that the dye X-GN has been completely oxidized into harmless final products such as H_2O and CO_2. Therefore, it is necessary to study TOC removal of X-GN. From the experimental results (Fig. 14), It was found that the two processes were more beneficial for decolorization rather than for TOC removal. After 140 min of irradiation over 98% color removal was achieved for heterogeneous photo-Fenton process while TOC removal was just 52.9%. But for visible light/H_2O_2/Fe^{3+} process,

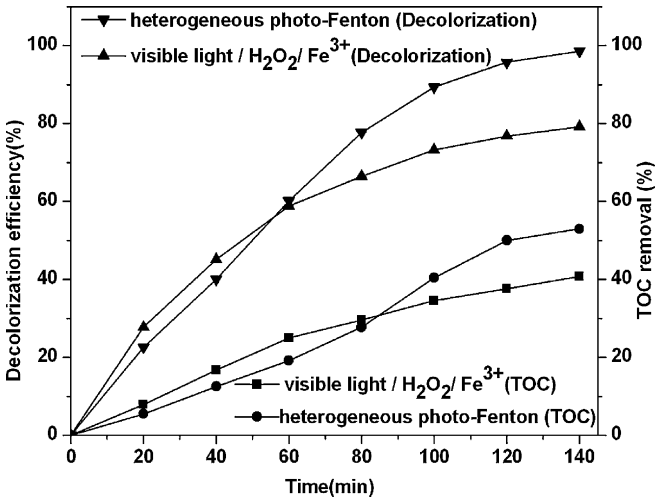

Fig. 14. Decolorization and mineralization as a function of time for a solution of X-GN by heterogeneous photo-Fenton and visible light/H_2O_2/Fe^{3+} processes.

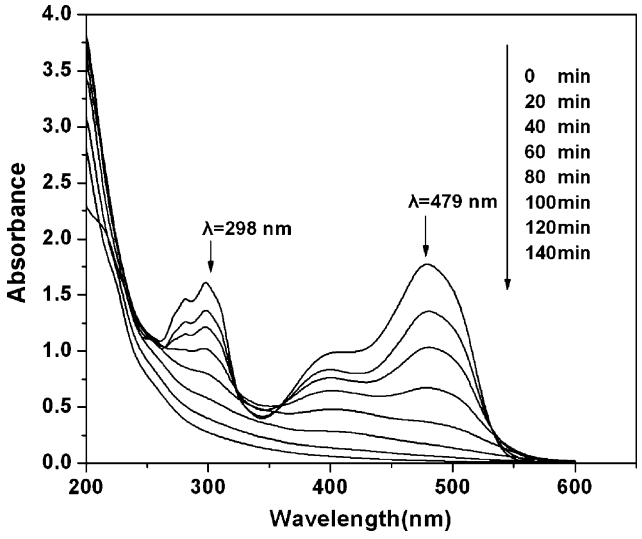

Fig. 15. UV–vis spectra of the 100 mg/L X-GN solution in heterogeneous photo-Fenton process. The experiments were conducted under conditions: [X-GN] = 100 mg/L, $[H_2O_2]_0$ = 4.9mmol/L, Fe-Mt = 0.6 g/L, pH 3, T = 30 °C.

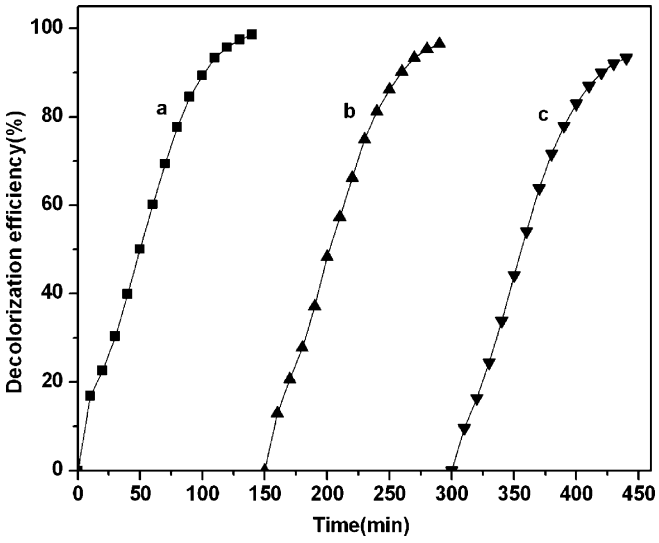

Fig. 16. Cycling runs in the decolorization of X-GN by heterogeneous photo-Fenton process: (a) the first run; (b) the second run; (c) the third run. The experiments were conducted under conditions: [X-GN] = 100 mg/L, $[H_2O_2]_0$ = 4.9mmol/L, Fe-Mt = 0.6 g/L, pH 3, T = 30 °C.

TOC removal of X-GN was lower effective, and only 40.7 removal percentage was attained.

3.3. The analysis of reaction products in heterogeneous photo-Fenton process

The absorption spectra of X-GN were scanned in the range 200–600 nm. The peak at 479 nm was attributed to the absorption of the $n \rightarrow \pi^*$ transition related to the –N=N– group, while another band at 298 nm was attributed to the $\pi \rightarrow \pi^*$ transition of the naphthalene ring in the X-GN molecule [22,28]. From Fig. 15, we can see that the characteristic absorption band of X-GN at 479 nm and 298 nm decreased rapidly following photolysis, and the former disappeared after 140 min of visible irradiation. The phenomenon can be explained as OH radicals produced in heterogeneous photo-Fenton process attacking the azo groups and opening the –N=N– bonds first, and then destroying the long conjugated π^* systems, thus causing decolorization.

However, there is strong absorbance in the range of 200–250 nm, which means that some intermediates exist after degradation of X-GN by heterogeneous photo-Fenton process.

3.4. The stability of iron-pillared montmorillonite catalyst

3.4.1. Long-term stability

The long-term stability of the Fe-Mt catalyst was tested by contacting fresh X-GN solutions with used catalyst from previous runs for the decolorization of X-GN under identical reaction conditions. The procedures that recycled the used Fe-Mt was as follows: Fe-Mt remained in the reaction solution was separated by centrifugation, and then washed with de-ionized water two times, dried at 80 °C for 24 h; the dried powder was used as a catalyst. As can be observed in Fig. 16, about 99% decolorization efficiency of X-GN was achieved within 140 min of irradiation in the first run (curve a). In the second run (curve b), 97% decolorization of X-GN was achieved and the third run (curve c) gave approximately 93% color removal. The results indicated that Fe-Mt retained most of its catalytic activity for at least three uses. Fe-Mt catalyst may have long-term stability.

3.4.2. Catalyst stability at various pH

Stability is an important property for an effective catalyst. Fig. 17 shows the concentrations of dissolved iron ions as a function of time

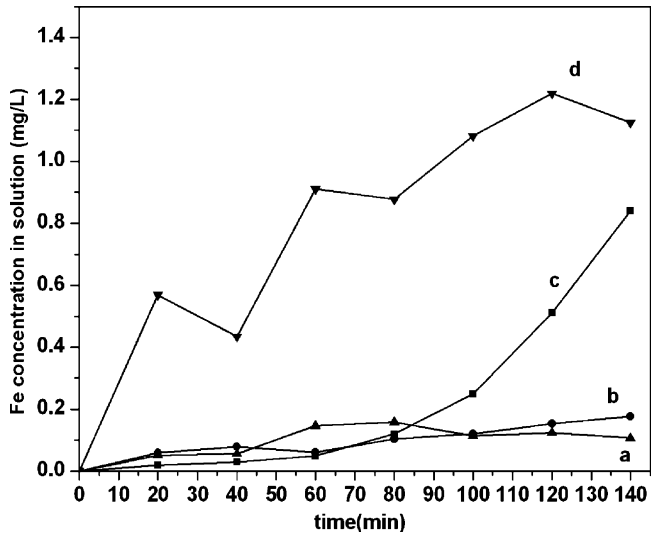

Fig. 17. Dissolved iron concentration as a function of time at different pH values in heterogeneous photo-Fenton process: (a) pH 5, (b) pH 4, (c) pH 3, (d) pH 2. The experiments were conducted under conditions: [X-GN] = 100 mg/L, $[H_2O_2]_0$ = 4.9 mmol/L, Fe-Mt = 0.6 g/L, T = 30 °C.

for pH between 2 and 5 in heterogeneous photo-Fenton process. At reaction times up to the completion of the experiment at 140 min at pH 3, the concentrations of iron ion in the solution remained are not more than 0.84 mg/L (curve c). The maximum metallic leaching level during reaction corresponds to 1.26% of the total iron in this catalyst. When the experiments were conducted at other pH values, as expected, the concentrations of dissolved iron (curve a and b) are all much lower than 0.84 mg/L except for some one at pH 2 (curve d). These results indicate that there is a strong interaction between iron ions and montmorillonite layers and the Fe-Mt is quite stable and thus can be in practice used for more operation cycles.

4. Conclusions

Based on a study of decolorization of reactive brilliant orange X-GN by a heterogeneous photo-Fenton process using iron-pillared montmorillonite (Fe-Mt) as the catalyst under visible irradiation,

the following conclusions have been drawn:

(1) Decolorization of X-GN can be induced by using Fe-Mt as a heterogeneous photo-Fenton catalyst under visible irradiation. Under the conditions of a reaction temperature of 30 °C, pH 3.0, 4.9 mmol/L H_2O_2 and 0.6 g/L catalyst after 140 min treatment under visible irradiation, 98.6% decolorization was achieved while 52.9% TOC removal was attained.
(2) UV–vis spectra of the degradation of X-GN showed that the intensity of the 484 nm and 298 nm absorption peaks decreased rapidly following photolysis, which was attributed to the absorption of the $n \rightarrow \pi^*$ transition related to the –N=N– group and the $\pi \rightarrow \pi^*$ transition of the naphthalene ring in X-GN molecule, respectively.
(3) The experiments of long-term stability showed that Fe-Mt retained almost all of its catalytic activity after reuse. Furthermore, the concentration of iron ions in the solution after the degradation reaction at 140 min corresponds to only 1.26% of the total iron content in the Fe-Mt catalyst. The low level of leaching shows that this can be a promising catalyst for industrial wastewater treatment.
(4) The use of a halogen lamp as light source showed that the heterogeneous photo-Fenton reaction is successful under visible radiation.

Acknowledgements

The authors are grateful for financial support from the National Science Foundation of China (Grant No. 40573064, 40202007), New Century Excellent Talents Program, Ministry of Education, China (Grant No. NCET-06-0747), Science and Technology Plan of Guangdong Province, China (Grant No.2006B36601004, 2008B030302036) and the Natural Science Foundation of Guangdong Province, China (Grant No. 06025666, 04020017). The authors thank Jim Irish at South China University of Technology (SCUT), China, for his English corrections.

References

[1] P.A. Carneiro, R.F. Pupo Nogueira, M.V.B. Zanoni, Homogeneous photodegradation of C.I. Reactive Blue 4 using a photo-Fenton process under artificial and solar irradiation, Dyes Pigm. 74 (2007) 127–132.
[2] C.G. Silva, W.D. Wang, J.L. Faria, Photocatalytic and photochemical degradation of mono-, di- and tri-azo dyes in aqueous solution under UV irradiation, J. Photochem. Photobiol. A: Chem. 181 (2006) 314–324.
[3] P. Nigam, I.M. Banat, D. Singh, R. Merchant, Microbial process for the decolourization of textile effluent containing azo, diazo and reactive dyes, Process Biochem. 31 (1996) 435–442.
[4] Y.M. Li, Y.Q. Lu, X.L. Zhu, Photo-Fenton discoloration of the azo dye X-3B over pillared bentonites containing iron, J. Hazard. Mater. B132 (2006) 196–201.
[5] D. Li, T. Yuranova, P. Albers, J. Kiwi, Accelerated photobleaching of Orange II on novel ($H_5FeW_{12}O_{40}10H_2O$)/silica structured fabrics, Water Res. 38 (2004) 3541–3550.
[6] K. Hanna, T. Kone, G. Medjahdi, Synthesis of the mixed oxides of iron and quartz and their catalytic activities for the Fenton-like oxidation, Catal. Commun. 9 (2008) 955–959.
[7] M. Tekbas, H.C. Yatmaz, N. Bektas, Heterogeneous photo-Fenton oxidation of reactive azo dye solutions using iron exchanged zeolite as a catalyst, Micropor. Mesopor. Mater. 115 (2008) 594–602.
[8] H. Kušić, N. Koprivanac, I. Selanec, Fe-exchanged zeolite as the effective heterogeneous Fenton-type catalyst for the organic pollutant minimization: UV irradiation assistance, Chemosphere 65 (2006) 65–73.
[9] J.H. Ramirez, C.A. Costa, L.M. Madeira, G. Mata, M.A. Vicente, M.L. Rojas-Cervantes, A.J. López-Peinado, R.M. Martín-Aranda, Fenton-like oxidation of Orange II solutions using heterogeneous catalysts based on saponite clay, Appl. Catal. B: Environ. 71 (2007) 44–56.
[10] X.L. Guo, Y.D. Yao, G.F. Yin, Y.Q. Kang, Y. Luo, L. Zhuo, Preparation of decolorizing ceramsites for printing and dyeing wastewater with acid and base treated clay, Appl. Clay Sci. 40 (2008) 20–26.
[11] M.A. De León, J. Castiglioni, J. Bussi, M. Sergio, Catalytic activity of an iron-pillared montmorillonitic clay mineral in heterogeneous photo-Fenton process, Catal. Today 133–135 (2008) 600–605.
[12] J. Feng, X. Hu, P.L. Yue, Novel bentonite clay-based Fe-nanocomposite as a heterogeneous catalyst for photo-Fenton discoloration and mineralization of Orange II, Environ. Sci. Technol. 38 (2004) 269–275.
[13] J.X. Chen, L.Z. Zhu, Heterogeneous UV-Fenton catalytic degradation of dyestuff in water with hydroxyl-Fe pillared bentonite, Catal. Today 126 (2007) 463–470.
[14] Y.F. Wang, W.H. Ma, C.C. Chen, X.F. Hu, J.C. Zhao, J.C. Yu, Fe^{3+}/Fe^{2+} cycling promoted by Ta_3N_5 under visible irradiation in Fenton degradation of organic pollutants, Appl. Catal. B: Environ. 75 (2007) 256–263.
[15] M.M. Cheng, W.J. Song, W.H. Ma, C.C. Chen, J.C. Zhao, J. Lin, H.Y. Zhu, Catalytic activity of iron species in layered clays for photodegradation of organic dyes under visible irradiation, Appl. Catal. B: Environ. 77 (2008) 355–363.
[16] E.G. Rightor, M.S. Tzou, T.J. Pinnavaia, Iron oxide pillared clay with large gallery height: synthesis and properties as a Fischer-Tropsch catalyst, J. Catalysis. 130 (1991) 29–40.
[17] P. Yuan, F. Bergaya, Q. Tao, M.D. Fan, A combined study by XRD, FTIR, TG and HRTEM on the structure of delaminated Fe-intercalated/pillared clay, J. Colloid Interf. Sci. 324 (2008) 142–149.
[18] J.H. Ma, W.J. Song, C.C. Chen, W.H. Ma, J.C. Zhao, Y.L. Tang, Fenton degradation of organic compounds promoted by dyes under visible irradiation, Environ. Sci. Technol. 39 (2005) 5810–5815.
[19] M.M. Cheng, W.H. Ma, J. Li, Y.P. Huang, J.C. Zhao, Y.X. Wen, Y.M. Xu, Dye pollutants over Fe(III)-loaded resin in the presence of H_2O_2 at neutral pH values, Environ. Sci. Technol. 38 (2004) 1569–1575.
[20] J. Herney Ramirez, C.A. Costa, L.M. Madeira, G. Mata, M.A. Vicente, M.L. Rojas-Cervantes, A.J. López-Peinado, R.M. Martín-Aranda, Fenton-like oxidation of Orange II solutions using heterogeneous catalysts based on saponite clay, Appl. Catal. B: Environ. 71 (2007) 44–56.
[21] H.L. Zheng, Y.X. Pan, X.Y. Xiang, Oxidation of acidic dye Eosin Y by the solar photo-Fenton processes, J. Hazard. Mater. 141 (2007) 457–464.
[22] M. Muruganandham, M. Swaminathan, Decolorization of reactive orange 4 by Fenton and photo-Fenton oxidation technology, Dyes Pigm. 63 (2004) 315–321.
[23] B.G. Kwon, D.S. Lee, N. Kang, J. Yoon, Characteristics of *p*-chlorophenol oxidation by Fenton's reagent, Water Res. 33 (1999) 2110–2118.
[24] M. Neamlu, C. Zaharia, C. Catrinescu, A. Yediler, M. Macoveanu, A. Kettrup, Fe-exchanged, Y zeolite as catalyst for wet peroxide oxidation of reactive azo dye *Procion Marine H-EXL*, Appl. Catal. B: Environ. 48 (2004) 287–294.
[25] J.Y. Feng, X.J. Hu, P.L. Yue, H.Y. Zhu, G.Q. Lu, Discoloration and mineralisation of reactive red HE-3B by heterogeneous photo-Fenton reaction, Water Res. 37 (2003) 3776–3784.
[26] J. Fernandez, J. Bandara, A. Lopez, Ph. Buffar, J. Kiwi, Photoassisted Fenton degradation of nonbiodegradable azo dye (Orange II) in Fe-free solutions mediated by cation transfer membranes, Langmuir 5 (1999) 185–192.
[27] J.H. Sun, S.P. Sun, M.H. Fan, H.Q. Guo, Y.F. Lee, R.X. Sun, Oxidative decomposition of *p*-nitroaniline in water by solar photo-Fenton advanced oxidation process, J. Hazard. Mater. 153 (2008) 187–193.
[28] F. Wu, N.S. Deng, H.L. Hua, Degradation mechanism of azo dye C. I. reactive red 2 by iron powder reduction and photooxidation in aqueous solutions, Chemosphere 41 (2000) 1233–1238.